

Highlights

Reducing RES Droughts through the integration of wind and PV

Boris Morin, Aina Maimo Far, Damian Flynn, Conor Sweeney

- Energy droughts are defined as periods of low production
- Three models compared to evaluate renewable energy droughts in Ireland
- Analysis of 45 years of ERA5 weather data for energy drought trends
- Diverse energy mix reduces drought frequency and duration significantly
- Model choice impacts energy drought results

Reducing RES Droughts through the integration of wind and PV

Boris Morin^a, Aina Maimo Far^a, Damian Flynn^b, Conor Sweeney^a

^a*University College Dublin, School of Mathematics and Statistics, , Dublin, , Ireland*

^b*University College Dublin, School of Electrical and Electronic Engineering, , Dublin, , Ireland*

Abstract

The dependence of renewable energy sources (RES) such as wind and photovoltaic (PV) systems on the weather poses a critical challenge for energy systems. This study investigates the impact of targeting a balanced distribution of wind and PV capacity on reducing periods of low renewable generation, known as RES droughts. Three different RES models are used to estimate the capacity factors for different installed capacities of wind and PV energy. The skill of the RES models is quantified by comparing capacity factor time series to observed data. Their skill at representing RES droughts is also quantified. The RES models are used to generate a 45-year hourly time series of RES generation, enabling analysis of the frequency, duration and return periods of RES droughts at a climatological scale. Results show the importance of using an accurate, validated RES model for RES drought risk assessment. The addition of PV capacity to a wind-dominated system results in a large reduction in the frequency and duration of RES droughts, as well as reducing seasonal drought patterns. These findings underscore the importance of diversification in RES capacity to enhance energy security and resilience.

Keywords: RES Drought, Wind Power, Solar PV Power, Renewable Energy Sources, Return Periods

1. Introduction

The EU aims to generate at least 69% of its electricity from renewable energy sources (RES) by 2030, up from 41% in 2022 ?. While this transition is essential for reducing greenhouse gas emissions, it also highlights the

5 challenge of managing the variability of weather-dependent energy sources
6 such as wind and photovoltaic (PV) power. This challenge is compounded
7 by the increasing electrification of energy sectors, which places greater de-
8 mand on the power system and makes it more sensitive to meteorological
9 conditions ????. Periods of low renewable generation, known as *Dunkelflaute*
10 or RES droughts, pose significant risks to system adequacy and energy secu-
11 rity, emphasizing the need for a resilient energy system to meet both growing
12 electricity demand and decarbonization targets.

13 This study focuses on Ireland, a region with a strong reliance on wind
14 power, which has ambitious targets for PV power expansion. This case study
15 provides valuable insights into the potential benefits of diversifying the re-
16 newable energy mix on RES droughts. The performance of different RES
17 models are compared, and a 45-year time series of RES generation is pro-
18 duced. The results highlight the role of increased PV capacity in reducing
19 RES drought risks, offering insights for policymakers and energy planners.

20 For this study, a RES drought event is defined as occurring when the
21 average capacity factor (CF) remains below a fixed threshold for a given
22 duration, following the methodology used in other research ????. Alterna-
23 tive methods exist for defining RES droughts. One approach uses relative
24 CF thresholds that change over the year to account for seasonal variations
25 in renewable energy generation ??????. Another common method relies on
26 percentile-based thresholds, where drought events are defined by identifying
27 periods of unusually low generation relative to historical production levels,
28 typically based on the lowest production percentiles ??. Additionally, some
29 studies combine these definitions with metrics that incorporate the demand
30 side of energy consumption, analysing the balance between supply and de-
31 mand during drought periods ????. In this paper, the focus is exclusively on
32 energy generation, and a fixed threshold approach to define RES droughts
33 is used, which facilitates consistent inter-comparison between scenarios with
34 different installed wind and PV capacities.

35 RES droughts are identified using onshore wind and PV CF time series. In
36 this study, three different datasets are used, all of which are driven by ERA5
37 data ?. Two of the datasets are part of C3S Energy (C3S-E) ?, an energy-
38 based operational dataset produced by the EU Copernicus Climate Change
39 Service ?. One of the C3S-E datasets provides CF time series aggregated
40 at the national scale, while the other provides the CF time series at each
41 grid point, at the ERA5 resolution of 0.25°. The third dataset was generated
42 using the Atlite model ?, which converts the ERA5 atmospheric data to a

43 generation time series using specified wind turbine and PV panel models.
44 Atlite is an open-source tool developed by PyPSA ? and is widely used for
45 estimating wind and PV generation ????.

46 The datasets used in this study are detailed in section 2, which describes
47 their characteristics and relevance for evaluating RES droughts. Section 3
48 outlines the RES models used to simulate wind and PV generation and pro-
49 vides the methodology for defining and identifying RES drought events, in-
50 cluding the thresholds and metrics applied. In section 4, the models are first
51 verified against observed energy data to assess their accuracy, followed by an
52 analysis of RES drought occurrences for two scenarios with different ratios
53 of installed wind to PV capacities. Finally, section 5 offers a discussion of
54 the results in the context of energy reliability and future planning, followed
55 by the main conclusions and recommendations for further research.

56 2. Data

57 This study uses publicly available datasets to construct and validate the
58 models for estimating the CF of wind and PV energy. The primary data
59 sources include: EirGrid and SONI, the transmission system operators (TSO)
60 for the Republic of Ireland and Northern Ireland, respectively; the ERA5
61 reanalysis dataset; and the C3S-E datasets.

62 2.1. Wind and PV Capacity Factor

63 EirGrid, the TSO for the Republic of Ireland, and SONI, the Northern
64 Ireland TSO, provide detailed datasets on all wind and PV farms across the
65 island of Ireland (Republic of Ireland and Northern Ireland) from 1990 to the
66 present ?. These datasets include information such as each farm’s installed
67 capacity, name, and connection date. To enhance the accuracy of this data,
68 the longitude and latitude for each farm were manually determined through
69 online searches. For simplicity, this data will be referred to as originating
70 from EirGrid, as all-island data was directly obtained from EirGrid, and the
71 combined regions of the Republic of Ireland and Northern Ireland will be
72 referred to as Ireland throughout the remainder of this document.

73 The spreadsheet available from the EirGrid website contains two key vari-
74 ables: generation and availability. Generation is the energy that a RES farm
75 actually contributed to the grid, which may include limitations introduced
76 by the TSO to maintain grid stability, such as constraints and curtailment.
77 Availability represents the energy that would have been generated from a

RES farm if no grid constraints had been applied, making it representative of the weather-related response. Generation and availability values are available from 2014 onward for wind power and from 2018 onward for PV power, although PV availability data only became present in the Republic of Ireland in 2023. This study focuses on availability for all analyses.

2.2. Atmospheric Variables

Atlite and C3S-E datasets are driven by the ERA5 reanalysis [?], produced by the European Centre for Medium-Range Weather Forecasts (ECMWF). This global gridded dataset provides hourly atmospheric variables from 1940 to the present at a horizontal resolution of 0.25°. It is widely used for estimating PV and wind energy ^{????}. Table 1 lists the ERA5 variables used by Atlite and C3S-Energy.

Table 1: ERA5 variables used to calculate wind and PV generation

ERA5 name	variable
100 metre zonal and meridional wind speed	u_{100}, v_{100}
2 metre temperature	$t2m$
Surface net solar radiation	ssr
Surface solar radiation downwards	$ssrd$
Top of atmosphere incident radiation	$tisr$
Total sky direct solar radiation at surface	$fdir$

2.3. C3S Energy

The EU Copernicus Climate Change Service developed the C3S-E renewable energy dataset for Europe [?], using ERA5 atmospheric variables and weather-to-energy models. This dataset provides hourly CF for wind and PV energy from 1979 to the present. The data are available on the same grid as the ERA5 data, which has a horizontal resolution of 0.25°. The time series are also available for download at two aggregated scales: regional (NUTS 2) and national.

The C3S-E dataset estimates wind energy using wind speeds at 100 metres (u_{100}, v_{100}) and a standard turbine model, the Vestas V136/3450, with a fixed hub height of 100 meters. This choice is based on expert advice and the trend in wind turbine installation. The PV generation model used by C3S-E uses two ERA5 variables: surface solar radiation downwards ($ssrd$)

103 and air temperature ($t2m$). PV generation is calculated multiple times, us-
104 ing the same model with different azimuth and tilt angles. The results are
105 aggregated based on a statistical distribution of the module angles based on
106 the geographical location ?.

107 3. Methods

108 This study uses three datasets to analyse RES droughts across the island
109 of Ireland. Data downloaded from C3S-E were used to obtain two datasets:
110 one based on national-level data (C3S-E N), and another on grid-level data
111 (C3S-E G). The third dataset was computed using the Atlite model (Atlite).

112 3.1. C3S-Energy National

113 For national-level analyses, the aggregated CF time series provided by
114 C3S-E were used at two levels: Republic of Ireland (NUTS0: IE) and North-
115 ern Ireland (NUTS2: UKN0). These are based on the assumption by C3S-E
116 that RES generation occurs at every ERA5 grid point in Ireland. We com-
117 puted a weighted average of these, based on the installed capacity of each
118 one, to represent the total CF for Ireland.

119 3.2. C3S-E Gridded

120 The gridded dataset from C3S-E was used to create CF datasets which
121 account for the location of RES farms in Ireland. A list of the RES farms in
122 Ireland was compiled, including each farm’s latitude, longitude and installed
123 capacity. Using these coordinates, the nearest grid point on the C3S-E grid
124 was identified for each farm. The CF values from the C3S-E dataset corre-
125 sponding to these grid points were retrieved. A weighted average of the CF
126 values was calculated, with the installed capacity of each farm serving as the
127 weight, to construct the CF time series for Ireland. This process resulted in
128 a time series of RES generation for each energy source (wind and PV) for
129 Ireland, which takes the location of the RES farms into account.

130 3.3. Atlite

131 Atlite transforms weather data into energy data using the gridded ERA5
132 data and the locations of existing RES farms, as described in C3S-E G.
133 ERA5 data for wind speed at 100 metres (u_{100} , v_{100}) are used to calculate
134 wind generation, while the ERA5 radiation variables (ssr , $ssrd$, $tisr$, and
135 $fdir$) and air temperature ($t2m$) are used to calculate PV generation. A

key distinction between C3S-E and Atlite lies in their representation of wind turbines and PV panels. This study identifies the most appropriate wind turbine power curve to use from the 121 power curves made available by Renewables.ninja ?. The selection of a specific wind turbine and PV panel characteristics is further discussed and explained in section 4.1.

3.4. Energy Scenarios

In addition to analysing wind and PV generation separately, a combined CF was computed for each model by averaging wind and PV generation, weighted by their installed capacities at the end of 2023 (5.9 GW for wind power and 0.6 GW for PV power). This configuration is referred to as the 91W-9PV scenario, reflecting the distribution of 91% wind and 9% PV capacity. Given that PV capacity in Ireland is low in 2023, and to explore how a more balanced distribution of wind and PV capacities might impact RES droughts, this study also considered a second scenario, referred to as 57W-43PV, where the installed PV capacity is assumed to increase to 8.6 GW, while wind capacity rises to 11.45 GW. These values are based on targets outlined in the roadmap published by the 2024 Climate Action Plan ?. This study does not include offshore wind in the analysis. Recent reports suggest that even by 2030, Ireland is unlikely to have any significant new offshore wind farms, with projected offshore capacity expected to remain near zero using realistic scenarios ?.

New time series were generated for both the Atlite and C3S-E G PV models, incorporating a revised distribution of installed capacity across Ireland as specified in the roadmap. For wind power, the CF time series remains unchanged, as significant shifts in the location of wind farms are not expected. In total, twelve CF time series were analysed in this study, six for individual wind and PV CF (three models for each source) in the 91W-9PV scenario, and an additional six time series that include the combined CF for 91W-9PV and 57W-43PV scenarios across the different models.

It is important to note that the specific capacity values used in this study are illustrative and are not intended to reflect precise future realities. Instead, they serve to explore the impact of transitioning from a wind-dominated system (91W-9PV) to a more evenly distributed system (57W-43PV). This approach allows for a comparative analysis between the two scenarios, assessing how the balance of RES capacity affects the occurrence of RES droughts.

171 3.5. RES Drought Definition

172 In this study, a RES drought event was defined as occurring when the
 173 24-hour moving average of CF remains below a fixed threshold of 0.1 for
 174 a period of longer than 24 hours. The choice of this threshold is somewhat
 175 arbitrary, but aligns with similar studies on low renewable energy production
 176 ????. By using a 24-hour moving average, fewer but longer-lasting events
 177 were captured compared to using the raw CF time series, which can be more
 178 sensitive to short-term fluctuations. A fixed threshold approach was chosen
 179 in this study to enable consistent inter-comparison between datasets.

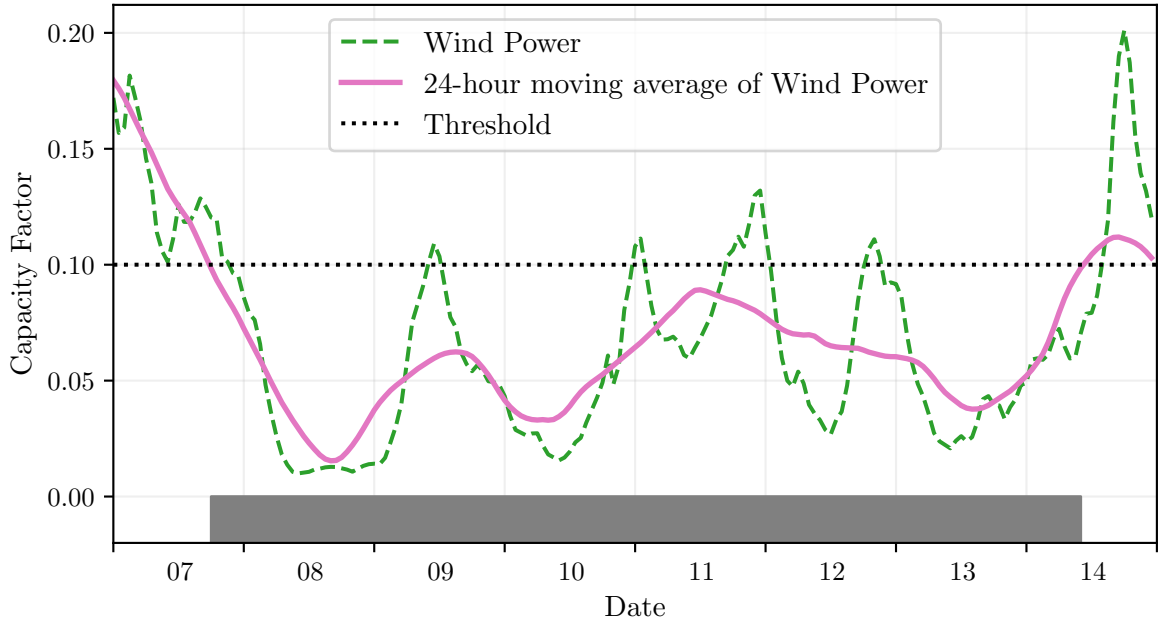


Figure 1: Wind time series of CF (green) and its 24-hour moving average (pink) from the 7th to the 15th of July 2021. The black dashed line indicates the CF threshold. The grey bar shows the period identified as a wind drought under our definition

180 The moving average approach smooths out short-term fluctuations, so
 181 that brief periods above the threshold do not interrupt an otherwise con-
 182 tinuous low-CF period (Fig. 1). This means that a single hour above the
 183 threshold does not "break" a drought event if it is surrounded by prolonged
 184 low-generation hours. As a result, fewer but longer-lasting drought events
 185 are identified, which may better reflect real-world conditions where energy
 186 supply constraints persist over extended periods.

187 4. Results

188 4.1. Verification

189 The accuracy of the datasets used in this study was verified, before con-
190 tinuing to the analysis of RES droughts. For the verification process, time-
191 varying values of installed capacity were used to account for changes in RES
192 development over the verification period. This step allowed us to assess how
193 well the datasets represent the production of renewable energy by comparing
194 them against observed data.

195 4.1.1. Wind Energy

196 The C3S-E datasets use the Vestas V136/3450 wind turbine power curve,
197 (Fig. 2a). The Atlite model allows the user to specify the power curve.
198 We considered the 121 power curves available for download from Renew-
199 ables.ninja ?. For each power curve, Renewables.ninja also provides four
200 associated smoothed power curves. The smoothing is done using a Gaus-
201 sian filter with different standard deviations that depend on the wind speed.
202 A separate wind CF time series for Ireland was generated for each of the
203 wind turbine power curves and smoothing levels. The performance of each
204 CF time series was then assessed based on four skill scores: correlation co-
205 efficient (CC), root mean square error (RMSE), mean bias error (MBE),
206 and area under the curve. The area under the curve was calculated from
207 histograms of the hourly CF values for the most recent decade, 2014-2023.
208 Based on these metrics, the most representative power curve for Ireland was
209 the Enercon E112.4500 power curve with the $0.3w$ smoothing filter.

210 The smoothing of the wind turbine power curve represents losses associ-
211 ated with each turbine, as well as losses such as wake effects between turbines,
212 which are important when modelling wind energy on larger spatial scales.
213 The histogram in Fig. 2b shows that the C3S-E power curve tends to under-
214 estimate low CF values and overestimate higher ones, whereas the smoothed
215 Atlite power curve more closely follows the recorded wind availability data
216 from EirGrid.

217 The effect of the difference between the power curves is also visible in
218 Fig. 3, which shows a density plot of wind CF values. The two C3S-E datasets
219 are shown to overestimate the observed CF, whereas the Atlite model is in
220 good agreement with the observed data. The skill scores presented in Table 2
221 show that Atlite performs better than the C3S-E datasets for all of the skill
222 scores.

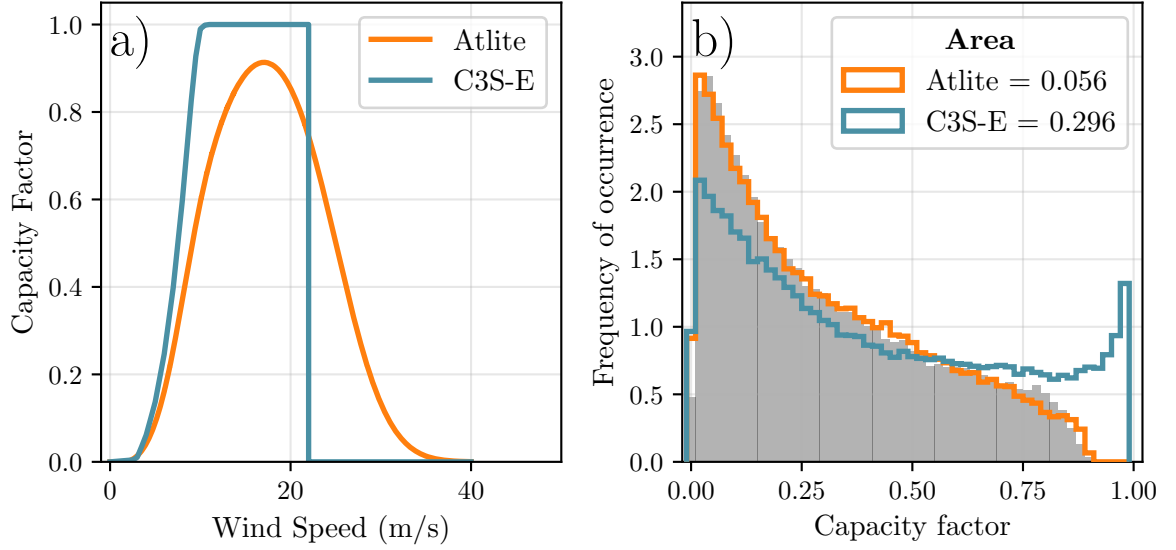


Figure 2: a) Power curves of the Enercon E112.4500 with a 0.3 smoothing filter used by Atlite (orange) and the Vestas V136/3450 used by C3S-E (teal) b) Histograms of wind CF for Ireland from Atlite (orange), C3S-E (teal) and Observed (shaded)

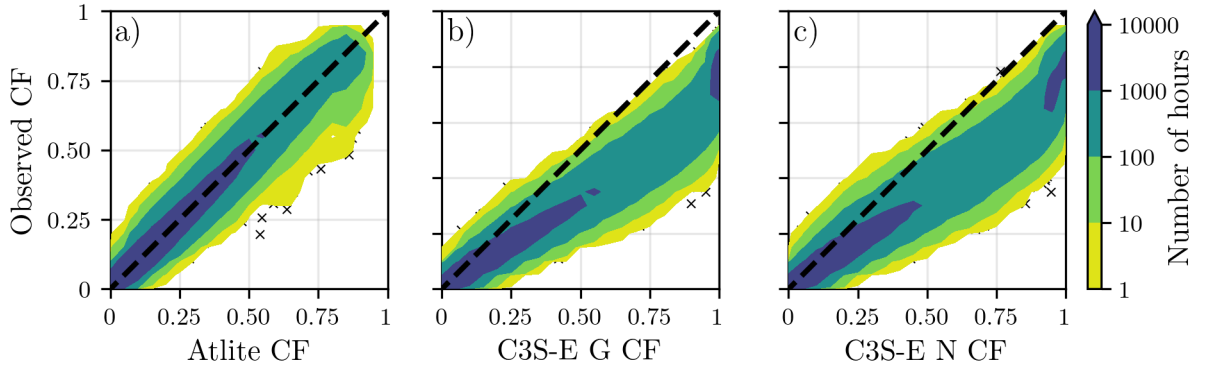


Figure 3: Wind CF density plot of the observed CF (vertical axes) and modelled (horizontal axes) CF data for the a) Atlite, b) C3S-E G and c) C3S-E N models

223 Fig. 4 presents the average annual number of wind drought events during
 224 the 2014 to 2023 validation period. The figure presents that Atlite shows
 225 the best agreement overall with the observed frequency and duration of wind
 226 drought events. This pattern is particularly evident for shorter-duration

	Atlite	C3S-E G	C3S-E N
CC	0.981	0.972	0.970
RMSE	0.045	0.177	0.162
MBE	-0.003	0.137	0.121

Table 2: Skill scores for wind power for the three datasets compared to observed data

227 events, which are the most frequent.

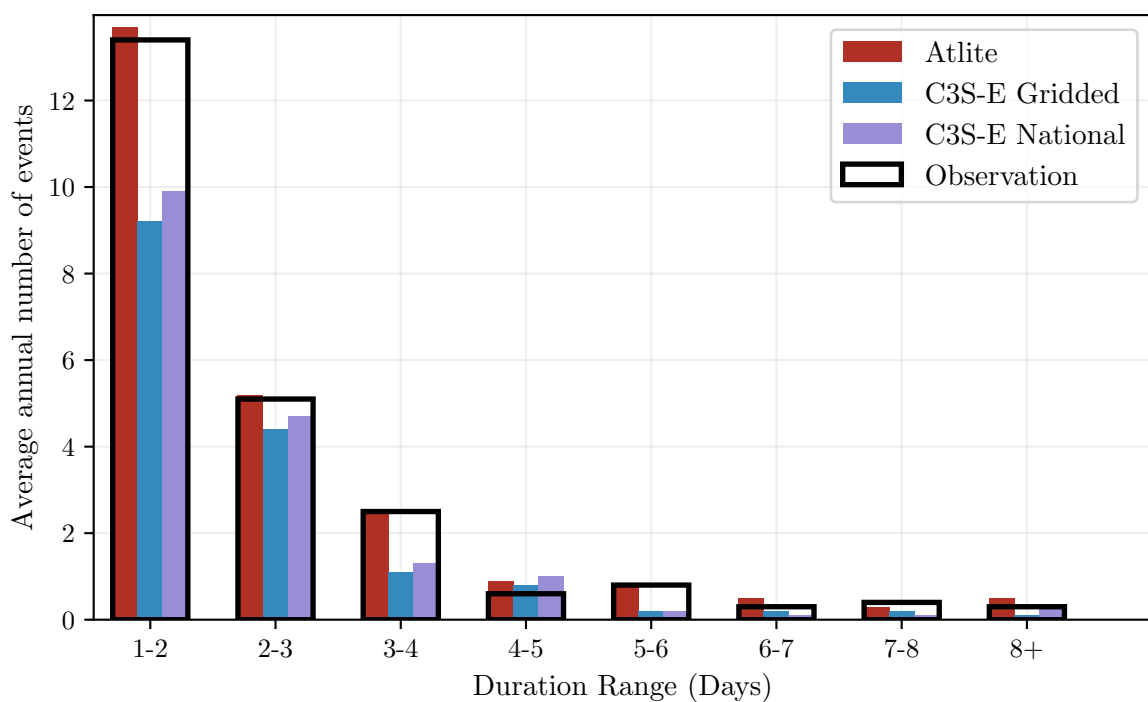


Figure 4: Average annual number of wind drought events for Atlite (red), C3S-E G (blue), C3S-E N (purple), and the observed data (black outline). The wind droughts are identified from 2014 to 2023

4.1.2. PV Energy

The Atlite model allows the user to select certain PV panel characteristics. In this study, the three PV panel types available in the Atlite model were considered (CSi, CdTe, Kaneka). Following the same methodology as in the previous section, the three available models were compared using four skill scores (CC, RMSE, MB, and area under the curve). Based on the best-performing metrics, the Breyer PV panel model was selected, using the Kaneka Hybrid panel option. For all PV farm locations, the azimuth angle is fixed at 180° (due south), and the optimal tilt angle option is applied.

The PV installed capacity available on the spreadsheets from EirGrid represents the Maximum Export Capacity (MEC) and does not accurately reflect the installed PV capacity. To enable actual PV generation potential to be modelled correctly, installed capacities were set at 1.4 times the MEC values. This scaling factor was estimated by analysing proprietary data from individual PV farms provided by EirGrid, which showed that the installed capacities of many farms exceed their MEC values by approximately 40%.

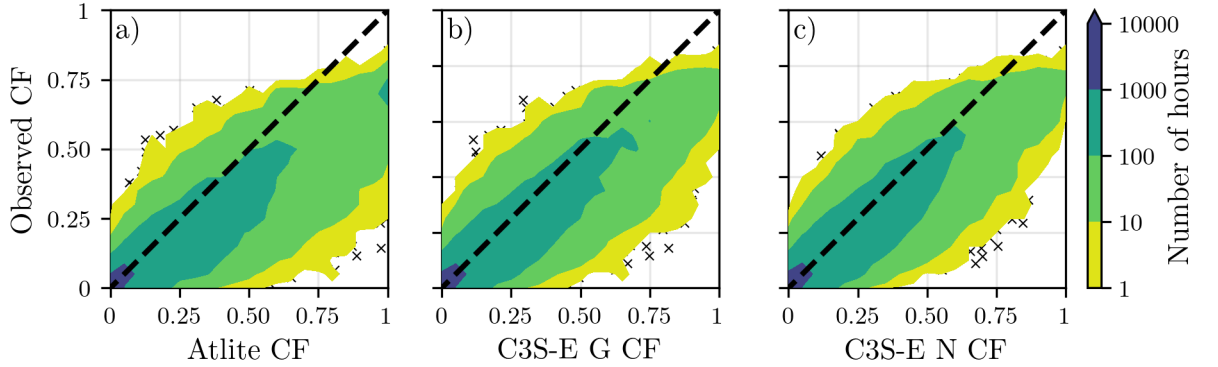


Figure 5: PV CF density plot of the observed (vertical axes) and modelled (horizontal axes) CF series for the a) Atlite, b) C3S-E G and c) C3S-E N models

Figure 5 shows that the three datasets have a similar tendency to overestimate the CF compared to the observed values, especially for high CF values. The skill scores presented in Table 3 indicate that C3S-E G performs best overall, with the lowest RMSE and a high correlation coefficient, suggesting a closer match to observed data. All models show a slight positive bias, with Atlite exhibiting a slightly lower correlation and higher RMSE.

Fig. 6 shows the number of PV drought events during the 2023 validation

	Atlite	C3S-E G	C3S-E N
CC	0.921	0.931	0.931
RMSE	0.119	0.090	0.113
MBE	0.046	0.027	0.021

Table 3: Skill scores for PV CF for the three datasets compared to observed data

251 period across different duration ranges. The figure reveals partial agreement
 252 between the three datasets and the observed data, with consistent results
 253 noticed for duration ranges of 1-2, 3-4, 7-8, and 8+ days. However, dis-
 254 crepancies appear in the other ranges, where the models diverge from the
 255 observed data. The main challenge in validating PV data stems from the
 256 recent installation of a large share of Ireland’s PV capacity, leading to un-
 257 certainties in PV generation data and the actual generating capacity in the
 258 first few months after each farm is connected. With over 65% of the total
 259 PV capacity installed in 2023, these data uncertainties significantly impact
 260 the ability to perform rigorous validation for PV drought events.

261 Nevertheless, the goal of this analysis is to assess the combination of wind
 262 and PV generation, where the complementary nature of these energy sources
 263 mitigates the limitations seen in PV-only results.

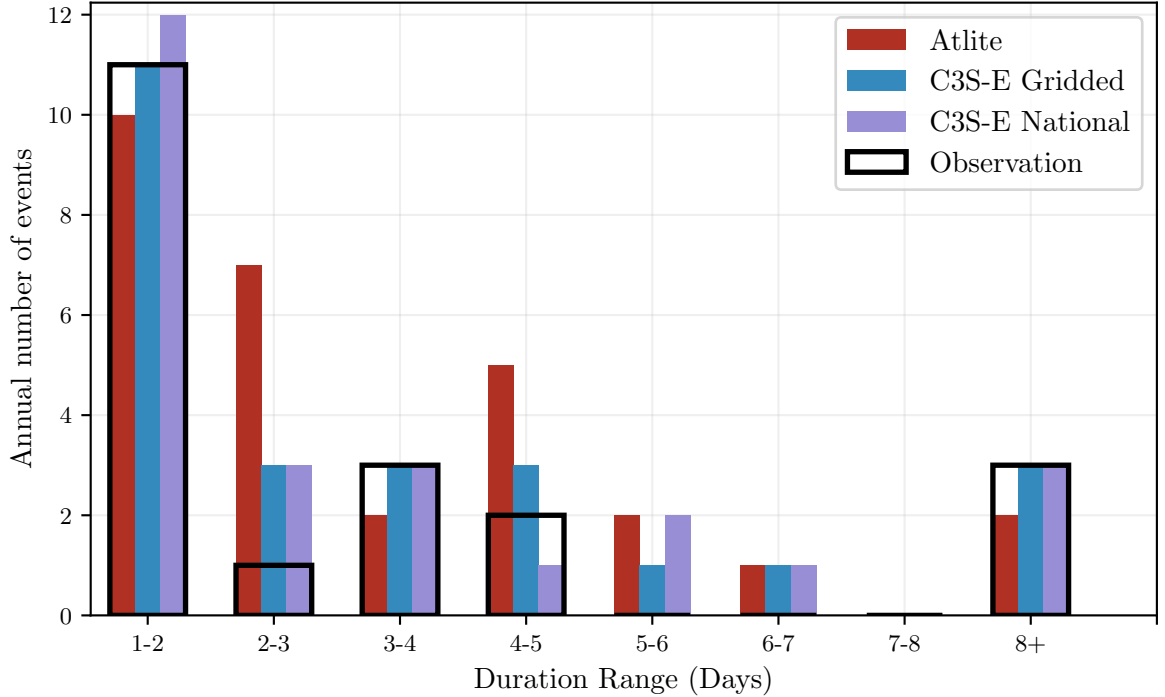


Figure 6: Number of PV drought events for Atlite (red), C3S-E G (blue), and C3S-E N (purple) and the observed data (black outline). The PV droughts are identified for 2023, considering the actual capacity of the system at any given time

264 4.2. Analysis

265 In this section, RES drought events are evaluated under two different
 266 scenarios with fixed installed capacities: the 91W-9PV scenario, with 5.9 GW
 267 of wind capacity and 0.6 GW of PV capacity, and the 57W-43PV scenario,
 268 where wind capacity comprises 11.45 GW and PV capacity increases to 8.6
 269 GW. Both scenarios were driven by 45 years of ERA5 data. Using the RES
 270 drought identification process described in Section 3.5, wind and PV droughts
 271 are first analysed separately before presenting the results for combined (wind
 272 + PV) RES droughts under both scenarios.

273 4.2.1. Annual Number of RES Droughts

274 The first part of the analysis examines the annual number of RES drought
 275 events across the three datasets. For Fig. 7a, the number of events decreases
 276 as the duration range increases, with very few events lasting more than seven

277 days. For Fig. 7b, the number of events also declines as the duration range
 278 extends from one to eight days, followed by a slight increase for longer dura-
 279 tions. This increase is due to extended low-generation periods occurring from
 280 November to March, depending on the dataset. When comparing wind and
 281 PV results (Fig. 7a & b), the median, first, and third quartiles for PV are
 282 consistently higher than or equal to those for wind, across all duration ranges
 283 and datasets. This is due to the typically lower CF of PV power compared
 284 to wind power, especially in a region such as Ireland where solar potential
 285 is limited. PV generation is also zero at night and constrained by the daily
 286 solar cycle, leading to a naturally higher frequency of RES droughts in PV
 287 compared to wind.

288 Fig. 7a & b show the combination of wind and PV under the two capacity
 289 scenarios. In the 91W-9PV scenario (Fig. 7c), the identified RES droughts
 290 closely match those for wind alone, which is expected due to the dominance
 291 of installed wind capacity. In contrast, the 57W-43PV scenario (Fig. 7d)
 292 shows a clear reduction in the number of drought events across all datasets
 293 and durations, with a decrease of the total number of events of 56% for Atlite,
 294 52% for C3S-E G, and 50% for C3S-E N. This reduction is attributed to the
 295 anti-correlation between wind and PV generation.

296 The median, first, and third quartiles for the Atlite dataset are consis-
 297 tently greater than or equal to those of the other two datasets, regardless of
 298 the duration range or type of renewable energy considered. This difference
 299 arises from the wind turbine power curve model used in the C3S-E datasets,
 300 which tends to overestimate the wind CF (Fig. 3). As a result, the overall
 301 number of RES droughts is underestimated in the C3S-E datasets compared
 302 to Atlite.

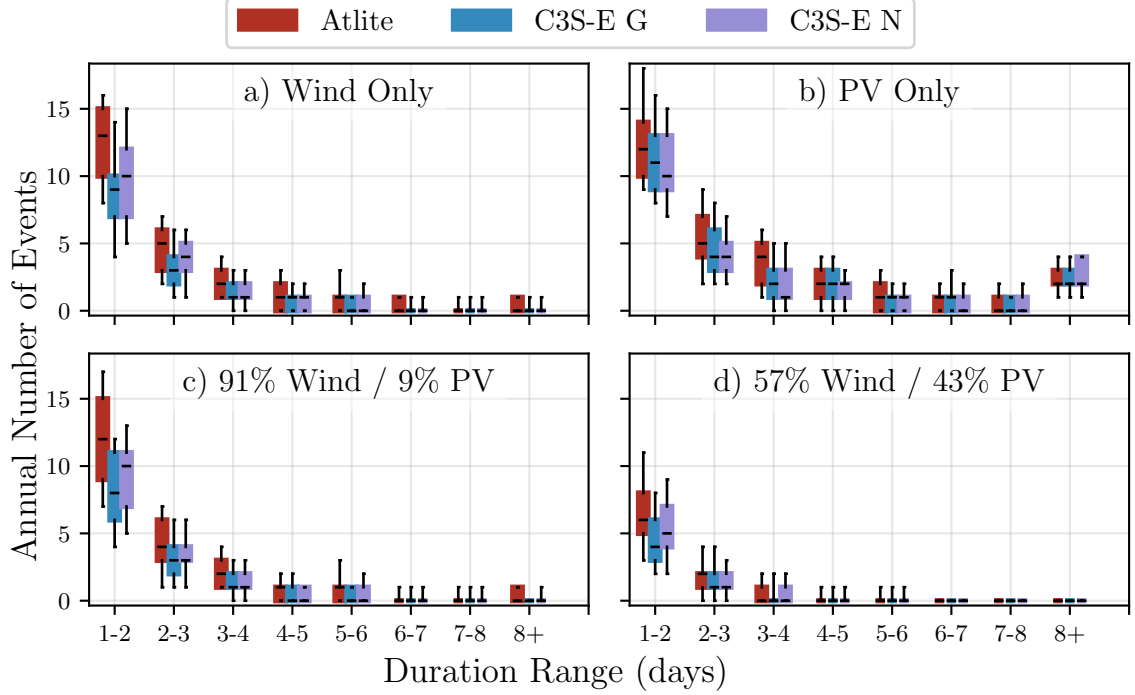


Figure 7: Annual number of RES droughts (from 1979 to 2023) for a) Wind, b) PV, and the combination for the c) 91W-9PV and d) 57W-43PV scenario for Atlite (red), C3S-E G (blue), and C3S-E N (purple). The x-axis represents duration ranges in days (lower bound included), while the y-axis indicates the annual number of events. The boxes display the first and third quartiles and the median is marked by a black line. The whiskers indicate the 5th and 95th percentiles

303 4.2.2. Return Periods of RES Drought Duration

304 The RES drought events identified over the 45-year period were used to
 305 calculate the return periods for different RES drought durations. A return
 306 period refers to the estimated expected interval between occurrences of events
 307 with a specified duration or intensity. Fig. 8 illustrates the return periods
 308 for varying RES drought durations, highlighting how often different drought
 309 lengths are likely to occur across the datasets. This analysis provides insight
 310 into the frequency and likelihood of prolonged low-generation periods, which
 311 is crucial for evaluating the potential impact of RES droughts on energy
 312 reliability and security of supply.

313 For wind (Fig. 8a), the duration of RES droughts increases in a log-

314 linear fashion across the three datasets. The log-linear trend indicates a pre-
315 dictable relationship between drought duration and occurrence, with longer
316 RES droughts becoming exponentially less likely as duration increases.

317 For PV (Fig. 8b), Atlite behaves differently than the two C3S-E datasets.
318 The Atlite results show a log-linear increase but reach higher values in general
319 with the longest event lasting forty days. For C3S-E G and C3S-E N, the
320 duration of RES droughts increases in a log-linear pattern for events lasting
321 less than 16 days. Beyond this duration, there is a sharp rise in drought
322 duration for events up to a one-year return period. This sudden increase
323 reflects the impact of winter on PV generation in Ireland, as PV output often
324 remains below the CF threshold for extended periods during winter months.
325 The difference between Atlite and the C3S-E results arises from differences in
326 the datasets near the threshold of 0.1 CF. Atlite remains slightly above the
327 threshold more frequently during these conditions, leading to shorter, more
328 fragmented drought events. In contrast, C3S-E G and C3S-E N tend to
329 fall below the threshold in similar conditions, resulting in longer continuous
330 drought periods, especially during winter. This sensitivity to the threshold
331 highlights how slight model differences can have substantial effects on drought
332 duration estimates, particularly for PV in low-generation conditions.

333 For the 91W-9PV scenario (Fig. 8c), the return periods mirror those of
334 Fig. 8a, due to the low levels of installed PV capacity. In the 57W-43PV
335 scenario (Fig. 8d), the return periods for RES droughts increase across all
336 durations. For example, the return period for a five-day drought event, shown
337 by the vertical dashed lines in Fig. 8, extends from roughly six months for
338 the 91W-9PV scenario, to four years for the 57W-43PV scenario in the Atlite
339 dataset, and from about fifteen months to around five years in the two C3S-E
340 datasets.

341 Across Fig. 8a, c, and, d, the return periods in the Atlite dataset are
342 consistently higher than those in the two C3S-E datasets. For instance, in
343 the 91W-9PV scenario (Fig. 8c), an event with a one-year return period
344 lasts six days in the Atlite dataset, compared to only five days in the C3S-E
345 datasets. This difference underscores the importance of model selection when
346 quantifying RES droughts, as each model’s assumptions and parametrisations
347 significantly influence drought duration estimates. Additionally, in all four
348 graphs, the similarity between results from the two C3S-E datasets suggests
349 that assumptions in the Atlite model—such as wind turbine power curve
350 selection and PV panel specifications—have a greater impact on RES drought
351 duration estimates than the precise geographic distribution of RES farms

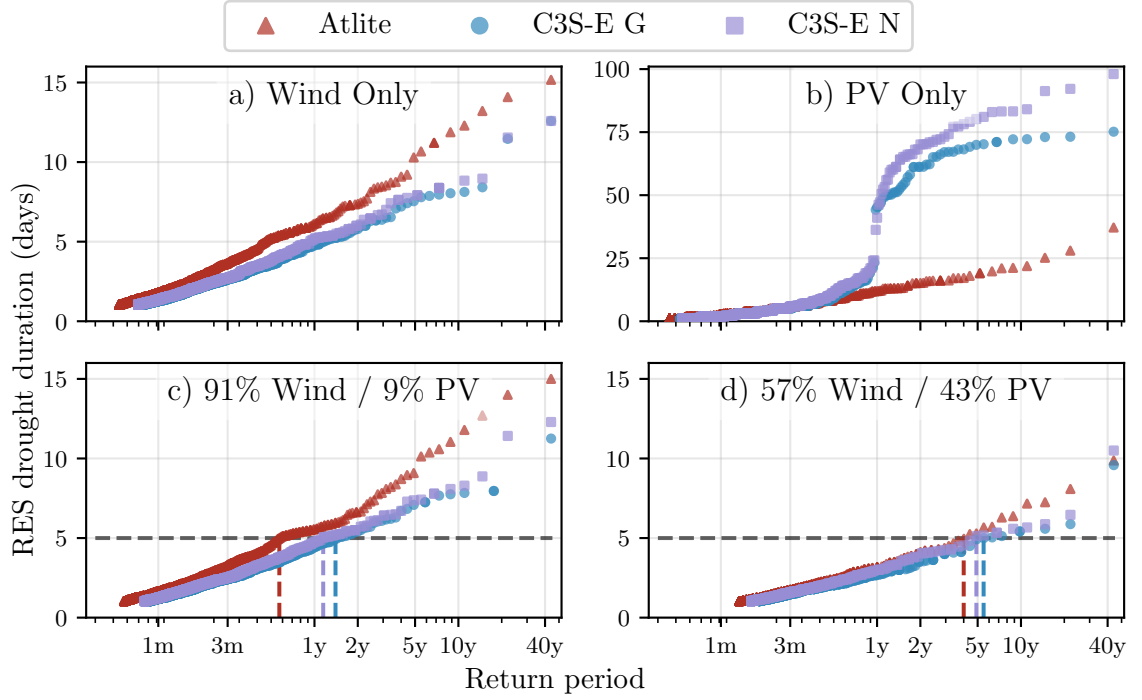


Figure 8: Return periods of the duration of RES droughts (from 1979 to 2023) for a) Wind, b) PV, and the combination for the c) 91W-9PV and d) 57W-43PV scenario, for Atlite (red triangle), C3S-E G (blue circle), and C3S-E N (purple square). The x-axis represents the return period time in a log-scale and the y-axis indicates the duration of RES drought associated with it. The horizontal dashed line marks the 5-day return period, with coloured vertical dashed marking its return period for each dataset

352 when studying the return periods of RES droughts.

353 4.2.3. Seasonal Distribution of RES Droughts

354 The seasonality of RES droughts was analysed by comparing the percent-
355 age of hours in each month classified as part of a RES drought.

356 For Fig. 9a, RES drought percentages are higher in summer than in win-
357 ter. In the Atlite dataset, for instance, an average of 24% of hours in summer
358 (June-July-August) are identified as RES droughts, compared to only 4% in
359 winter (December-January-February). This seasonal variation is influenced
360 by the wind power curve model used to estimate CF, where the shape of the
361 curve in lower wind speed regions (3-10 m/s) leads to significant differences
362 in CF under low wind conditions. In contrast, the results for Fig. 9b show
363 a higher percentage in winter, with RES droughts occurring over 60% of the
364 time regardless of the dataset. The Atlite results show a higher percent-
365 age of RES drought hours for wind, and a slightly lower percentage for PV,
366 compared to the two C3S-E datasets.

367 Similar to previous results, the 91W-9PV scenario (Fig. 9c) shows pat-
368 terns comparable to 9a. However, in the 91W/9PV scenario, the number of
369 hours classified as RES droughts in summer decreases slightly compared to
370 the wind-only scenario. This reduction can be explained by the contribution
371 of PV generation during the summer months in the 91W-9PV scenario, even
372 though it constitutes only 11% of total capacity. Since the number of RES
373 drought hours for PV in summer is near zero, this small contribution has a
374 noticeable impact on reducing overall drought hours. In the 57W-43PV sce-
375 nario (Fig. 9d), all three datasets show a reduction in monthly RES drought
376 frequency. Annual reductions in median RES drought frequency are observed
377 across the datasets, dropping from 14% to 5% for Atlite, from 8% to 3% for
378 C3S-E G, and from 9% to 4% for C3S-E N. The balanced mix of wind and
379 PV power in this scenario reduces the seasonal signal overall and significantly
380 decreases the percentage of RES drought hours in the summer.

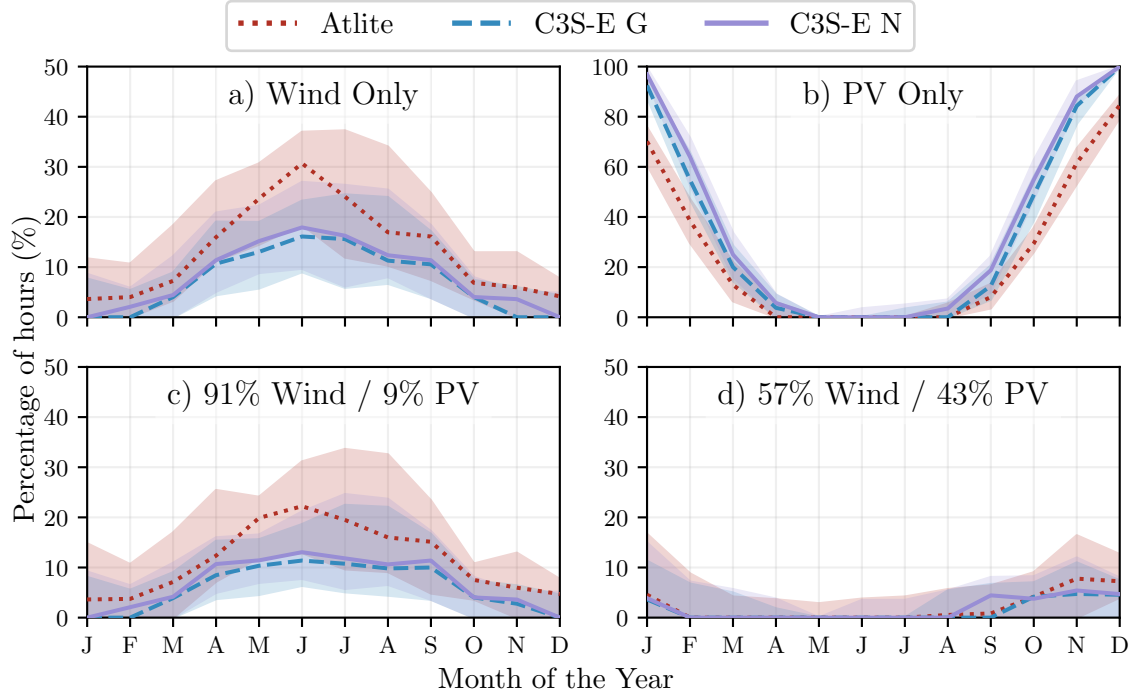


Figure 9: Percentage of hours in a month which are part of a RES drought (from 1979 to 2023) for a) Wind, b) PV, and the combination for the c) 91W-9PV and d) 57W-43PV scenario, for Atlite (red dotted), C3S-E G (blue dashed), and C3S-E N (purple solid). The x-axis represents the month of the year, and the y-axis indicates the percentage of hours. Lines correspond to the median values and the area between the first and third quartiles is shaded.

5. Discussion and Conclusions

This study has investigated the ability of three RES models to represent RES droughts: Atlite, C3S-E G, and C3S-E N. One of the most evident differences is how each dataset incorporates the specific locations of RES farms. Both Atlite and C3S-E G consider the locations of wind and PV farms, which should, in theory, provide a more accurate representation of RES generation. While this approach slightly improves PV models, our analysis indicates that for wind energy, the Atlite dataset performs better overall, especially in its close alignment with observed data for wind generation estimates. This finding suggests that, although the inclusion of RES farm locations is beneficial, the accuracy of the RES model is more strongly influenced by underlying

392 model assumptions, such as selecting an appropriate wind power curve.

393 Atlite shows the best alignment with observed data for wind generation.
394 Differences between the models are smaller for PV, with C3S-G performing
395 marginally better than the other two. The results show that the two C3S-
396 E datasets (C3S-E G and C3S-E N) consistently yield similar outcomes,
397 indicating that their methodological differences have minimal impact. This
398 distinction was also evident in the analysis, where Atlite reported higher
399 return periods and a greater number of RES droughts, especially in scenarios
400 with a balanced share of RES. Again, the results from RES drought modelling
401 rely more on the precision of the wind power curve and PV panel models
402 than on the specific locations of RES farms. Atlite’s superior performance
403 highlights the importance of selecting validated models for assessing RES
404 drought risks. This careful model selection can better quantify risks, support
405 effective planning, and avoid the potential underestimation of capacity needs,
406 which is essential for ensuring energy security.

407 Looking at the 57W-43PV scenario, the analysis showed a significant im-
408 provement in the management of RES droughts due to the complementary
409 nature of wind and PV generation. Wind and PV together perform better
410 in terms of reducing drought frequency and duration than either would in-
411 dividually, largely because of the seasonal anti-correlation between the two
412 energy sources. This diversification reduces the seasonal impact on RES
413 droughts, as PV generation peaks in the summer and wind generation is
414 more consistent in winter. Ireland currently has a highly wind-dependent
415 energy system, but with ambitious targets for PV installations in the coming
416 years, the energy mix is expected to approach a balance between wind and
417 PV capacity. While this balanced approach offers a more stable and secure
418 energy supply by mitigating RES drought risks, it is important to note that
419 having similar wind and PV capacities may not optimise other aspects, such
420 as annual energy production or meeting nighttime loads. For policymakers,
421 these findings underscore the importance of meeting these capacity targets
422 to enhance energy security through diversification. Additionally, the choice
423 of model for RES drought assessment becomes increasingly critical as more
424 renewable capacity is integrated into the system.

425 Future work is planned to extend the current analysis. First, climate pro-
426 jection data will be integrated with different energy scenarios, incorporating
427 the addition of offshore wind, to better understand how climate change might
428 affect RES droughts. Second, expanding the geographic domain of the study
429 to include the EU would provide a more comprehensive understanding of

430 RES droughts in an interconnected energy grid. This would require exten-
431 sive verification across all EU countries, making it a more complex but highly
432 relevant challenge.